

Approaching the full octave: Noncollinear optical parametric chirped pulse amplification with two-color pumping

D. Herrmann,^{1,2,*} C. Homann,² R. Tautz,^{1,3} M. Scharrer,⁴ P. St.J. Russell,⁴ F. Krausz,^{1,5}
L. Veisz,^{1,6} and E. Riedle²

¹ Max-Planck-Institut für Quantenoptik, Hans-Kopfermann-Str. 1, 85748 Garching, Germany

² LS für BioMolekulare Optik, LMU München, Oettingenstr. 67, 80538 München, Germany

³ present address: LS für Photonik und Optoelektronik, LMU München, Amalienstr. 54, 80799 München, Germany

⁴ Max-Planck-Institut für die Physik des Lichts, Günther-Scharowsky-Str. 1/Bau 24, 91058 Erlangen, Germany

⁵ LS für Laserphysik, LMU München, Am Coulombwall 1, 85748 Garching, Germany

⁶ laszlo.veisz@mpq.mpg.de

*d.herrmann@physik.uni-muenchen.de

Abstract: We present a new method to broaden the amplification range in optical parametric amplification toward the bandwidth needed for single cycle femtosecond pulses. Two-color pumping of independent stages is used to sequentially amplify the long and short wavelength parts of the ultrabroadband seed pulses. The concept is tested in two related experiments. With multi-mJ pumping pulses with a nearly octave spanning spectrum and an uncompressed energy of 3 mJ are generated at low repetition rate. The spectral phase varies slowly and continuously in the overlap region as shown with 100 kHz repetition rate. This should allow the compression to the Fourier limit of below 5 fs in the high energy system.

©2010 Optical Society of America

OCIS codes: (190.7110) Ultrafast nonlinear optics; (190.4970) Parametric oscillators and amplifiers; (190.2620) Harmonic generation and mixing; (320.5520) Pulse compression; (190.4975) Parametric processes; (260.7120) Ultrafast phenomena

References and links

1. F. Krausz, and M. Ivanov, "Attosecond physics," *Rev. Mod. Phys.* **81**(1), 163–234 (2009).
2. G. D. Tsakiris, K. Eidmann, J. Meyer-ter-Vehn, and F. Krausz, "Route to intense single attosecond pulses," *N. J. Phys.* **8**(1), 19 (2006).
3. T. Tajima, "Laser acceleration and its future," *Proc. Jpn. Acad. Ser. B* **86**(3), 147–157 (2010).
4. M. Nisoli, S. De Silvestri, and O. Svelto, "Generation of high energy 10 fs pulses by a new pulse compression technique," *Appl. Phys. Lett.* **68**(20), 2793–2795 (1996).
5. C. P. Hauri, W. Kornelis, F. W. Helbing, A. Heinrich, A. Couairon, A. Mysyrowicz, J. Biegert, and U. Keller, "Generation of intense, carrier-envelope phase-locked few-cycle laser pulses through filamentation," *Appl. Phys. B* **79**(6), 673–677 (2004).
6. G. M. Gale, M. Cavallari, T. J. Driscoll, and F. Hache, "Sub-20-fs tunable pulses in the visible from an 82-MHz optical parametric oscillator," *Opt. Lett.* **20**(14), 1562–1564 (1995).
7. T. Wilhelm, J. Piel, and E. Riedle, "Sub-20-fs pulses tunable across the visible from a blue-pumped single-pass noncollinear parametric converter," *Opt. Lett.* **22**(19), 1494–1496 (1997).
8. A. Baltuška, T. Fuji, and T. Kobayashi, "Visible pulse compression to 4 fs by optical parametric amplification and programmable dispersion control," *Opt. Lett.* **27**(5), 306–308 (2002).
9. S. Adachi, N. Ishii, T. Kanai, A. Kosuge, J. Itatani, Y. Kobayashi, D. Yoshitomi, K. Torizuka, and S. Watanabe, "5-fs, Multi-mJ, CEP-locked parametric chirped-pulse amplifier pumped by a 450-nm source at 1 kHz," *Opt. Express* **16**(19), 14341–14352 (2008).
10. I. N. Ross, P. Matousek, M. Towrie, A. J. Langley, and J. L. Collier, "The prospects for ultrashort pulse duration and ultrahigh intensity using optical parametric chirped pulse amplification," *Opt. Commun.* **144**(1-3), 125–133 (1997).
11. S. Witte, R. T. Zinkstok, A. L. Wolf, W. Hogervorst, W. Ubachs, and K. S. E. Eikema, "A source of 2 terawatt, 2.7 cycle laser pulses based on noncollinear optical parametric chirped pulse amplification," *Opt. Express* **14**(18), 8168–8177 (2006).
12. D. Herrmann, L. Veisz, R. Tautz, F. Tavella, K. Schmid, V. Pervak, and F. Krausz, "Generation of sub-three-cycle, 16 TW light pulses by using noncollinear optical parametric chirped-pulse amplification," *Opt. Lett.* **34**(16), 2459–2461 (2009).

13. T. S. Sosnowski, P. B. Stephens, and T. B. Norris, "Production of 30-fs pulses tunable throughout the visible spectral region by a new technique in optical parametric amplification," *Opt. Lett.* **21**(2), 140–142 (1996).
14. E. Zeromskis, A. Dubietis, G. Tamosauskas, and A. Piskarskas, "Gain bandwidth broadening of the continuum-seeded optical parametric amplifier by use of two pump beams," *Opt. Commun.* **203**(3-6), 435–440 (2002).
15. D. Herrmann, R. Tautz, F. Tavella, F. Krausz, and L. Veisz, "Investigation of two-beam-pumped noncollinear optical parametric chirped-pulse amplification for the generation of few-cycle light pulses," *Opt. Express* **18**(5), 4170–4183 (2010).
16. G. Tamošauskas, A. Dubietis, G. Valiulis, and A. Piskarskas, "Optical parametric amplifier pumped by two mutually incoherent laser beams," *Appl. Phys. B* **91**(2), 305–307 (2008).
17. C. Schriever, S. Lochbrunner, P. Krok, and E. Riedle, "Tunable pulses from below 300 to 970 nm with durations down to 14 fs based on a 2 MHz ytterbium-doped fiber system," *Opt. Lett.* **33**(2), 192–194 (2008).
18. C. Homann, C. Schriever, P. Baum, and E. Riedle, "Octave wide tunable UV-pumped NOPA: pulses down to 20 fs at 0.5 MHz repetition rate," *Opt. Express* **16**(8), 5746–5756 (2008).
19. M. Bradler, P. Baum, and E. Riedle, "Femtosecond continuum generation in bulk laser host materials with sub- μ J pump pulses," *Appl. Phys. B* **97**(3), 561–574 (2009).
20. G. Cerullo, M. Nisoli, S. Stagira, and S. De Silvestri, "Sub-8-fs pulses from an ultrabroadband optical parametric amplifier in the visible," *Opt. Lett.* **23**(16), 1283–1285 (1998).
21. I. Z. Kozma, P. Baum, U. Schmidhammer, S. Lochbrunner, and E. Riedle, "Compact autocorrelator for the online measurement of tunable 10 femtosecond pulses," *Rev. Sci. Instrum.* **75**(7), 2323–2327 (2004).
22. P. Baum, S. Lochbrunner, and E. Riedle, "Zero-additional-phase SPIDER: full characterization of visible and sub-20-fs ultraviolet pulses," *Opt. Lett.* **29**(2), 210–212 (2004).
23. S. Witte, R. T. Zinkstok, W. Hogervorst, and K. S. E. Eikema, "Numerical simulations for performance optimization of a few-cycle terawatt NOPCPA system," *Appl. Phys. B* **87**(4), 677–684 (2007).
24. A. L. Cavalieri, E. Goulielmakis, B. Horvath, W. Helml, M. Schultze, M. Fiess, V. Pervak, L. Veisz, V. S. Yakovlev, M. Uiberacker, A. Apolonski, F. Krausz, and R. Kienberger, "Intense 1.5-cycle near infrared laser waveforms and their use for the generation of ultra-broadband soft-x-ray harmonic continua," *N. J. Phys.* **9**(7), 242 (2007).
25. J. Park, J. H. Lee, and C. H. Nam, "Generation of 1.5 cycle 0.3 TW laser pulses using a hollow-fiber pulse compressor," *Opt. Lett.* **34**(15), 2342–2344 (2009).
26. A. Baltuška, and T. Kobayashi, "Adaptive shaping of two-cycle visible pulses using a flexible mirror," *Appl. Phys. B* **75**(4-5), 427–443 (2002).
27. I. N. Ross, P. Matousek, G. H. C. New, and K. Osvay, "Analysis and optimization of optical parametric chirped pulse amplification," *J. Opt. Soc. Am. B* **19**(12), 2945–2956 (2002).
28. A. Renault, D. Z. Kandula, S. Witte, A. L. Wolf, R. Th. Zinkstok, W. Hogervorst, and K. S. E. Eikema, "Phase stability of terawatt-class ultrabroadband parametric amplification," *Opt. Lett.* **32**(16), 2363–2365 (2007).
29. G. Rodriguez, and A. J. Taylor, "Measurement of cross-phase modulation in optical materials through the direct measurement of the optical phase change," *Opt. Lett.* **23**(11), 858–860 (1998).
30. G. Krauss, S. Lohss, T. Hanke, A. Sell, S. Eggert, R. Huber, and A. Leitensdorfer, "Synthesis of a single cycle of light with compact erbium-doped fibre technology," *Nat. Photonics* **4**(1), 33–36 (2010).

1. Introduction

High energy ultrafast light pulses are unique tools for applications ranging from the most fundamental science to medical applications. Quasi-single cycle near infrared pulses can generate single attosecond pulses or even single cycle attosecond pulses in the XUV that allow the measurement of the fastest known processes [1,2]. Even with slightly longer pump pulses highly attractive electron acceleration has been shown that offers a tabletop alternative to large scale facilities used in clinical environments [3].

With known laser materials used in multi-stage optically pumped chirped pulse amplifiers the attainable spectral width is limited by either the intrinsic gain bandwidth or even more severely the spectral gain narrowing in going from nJ broadband seed light to the desired Joule output levels. To overcome these limitations, frequency broadening in either gas filled hollow capillary fibers [4] or in filaments [5] is widely used. So far the use is, however, limited to at most a few mJ.

An attractive alternative for the direct generation of high energy extremely broadband pulses is optical parametric amplification. With a noncollinear geometry and pumping by a frequency-doubled femtosecond Ti:sapphire laser, sub-20 fs visible pulses have indeed been generated at 82 MHz repetition rate [6] and multi- μ J pulses at kHz rates [7]. The concept of the noncollinearly phase-matched optical parametric amplifier (NOPA) was optimized to the generation of 4 fs pulses [8].

Pumping by femtosecond Ti:sapphire pulses limits the attainable output energy, even though extremely short pulses with peak powers of 0.5 TW have been demonstrated [9]. Therefore the use of pico- or even nanosecond pump pulses was suggested in combination

with a chirped pulse strategy (OPCPA) [10]. All known and technically available pump lasers with ps pulse duration operate around 1050 nm due to the laser active materials used, e.g. Nd⁺ or Yb⁺. The use of such pump lasers has already led to 2 TW pulses [11] and lately sub-8 fs pulses centered at 805 nm with more than 130 mJ (16 TW) compressed energy [12]. A further shortening of the pulses in this spectral region becomes increasingly difficult due to the phase-matching bandwidth of the BBO amplifier medium with one-color pumping.

Already 1996 it was shown that multiple amplification stages with slight spectral detuning of the individual amplification range could lead to significant shortening of the output in a 100 kHz OPA [13]. Pumping of a single stage with multiple pump beams allowed the demonstration of pulse shortening from 98 to 61 fs [14] and lately from 8 to 7 fs with an improved temporal structure [15]. The use of different pump wavelengths was even suggested, yet no spectral nor temporal characterization of the output has been provided [16].

For a MHz Yb-based femtosecond pump system it was shown that both the green 2ω light and the UV 3ω light can be used to pump a NOPA [17,18]. Both configurations easily yield sub-20 fs pulse durations even without optimized compression. Interestingly, the 2ω pumping produces these pulses in the red and the 3ω pumping in the green and yellow part of the spectrum. We therefore suggest the simultaneous use of green and UV pumped stages together with a chirped pulse scheme and high energy pumping. This should allow the generation of pulses with unprecedented shortness and pulse energy.

In this communication we report on two pilot experiments that are aimed on testing this hypothesis. With tens of mJ pumping the generation of nearly octave-spanning few-mJ pulses is achieved. For this effort, techniques have been developed to allow efficient frequency conversion of the 78 ps fundamental pump pulses at 1064 nm. In a second experiment at 100 kHz repetition rate the compressibility and spectral phase behavior of the composite pulses is investigated.

2. NOPCPA on the mJ-level approaching the octave

Figure 1 shows the layout of the experimental two-color-pumped NOPCPA setup. We have extended an existing system (denoted as Light-Wave-Synthesizer-20, Ref. [12]), which generates sub-8 fs, 130-mJ pulses at 805 nm central wavelength and 10 Hz repetition rate.

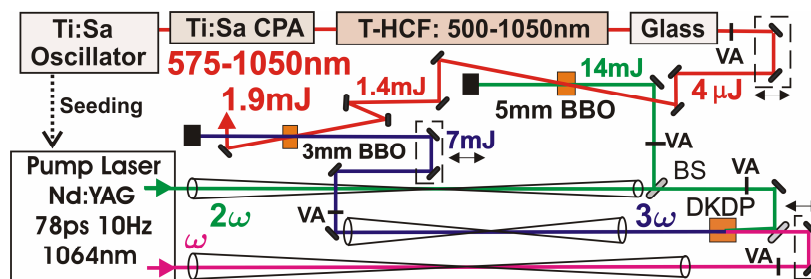


Fig. 1. Layout of the mJ-level two-color-pumped NOPCPA setup, which consists of two cascaded stages employing type-I phase-matching in BBO (T-HCF – tapered hollow-core capillary fiber, VA – variable attenuator, BS – beam splitter). The pump fundamental (1064 nm, ω) and its second- (532 nm, 2ω) and third-harmonic (355 nm, 3ω) are relay-imaged with vacuum telescopes onto the nonlinear optical crystals BBO and DKDP.

The present system consists of a Ti:sapphire master oscillator from which the broadband seed and the pump pulses for the two-stage NOPCPA chain are derived. 60% of the oscillator output is fed into a Ti:sapphire 9-pass chirped-pulse amplifier (Femtopower Compact pro, Femtolasers GmbH), delivering 25-fs, 800- μ J pulses at 1 kHz. After amplification, the pulses are spectrally broadened in a 1 m long tapered hollow-core capillary fiber (T-HCF) filled with neon gas at 2 bar (1500 Torr) absolute pressure, which leads to a seed spectrum ranging from 500 to 1050 nm (30 dB; see Fig. 2). The larger diameter of 500 μ m in the first 10 cm together with the small diameter of 200 μ m in the main part helps broaden the spectrum by up to

50 nm in the red wing. These pulses are then stretched in time by a variable amount of glass, leading to an adjustable group delay (GD) of the seed spectral boundaries. The seed pulse energy is attenuated to 4 μJ to be comparable with the seed used in Ref. [12].

The remaining 40% of the oscillator output is used to seed the Nd:YAG pump laser (EKSPLA, UAB), providing all-optical synchronization. This pump laser delivers two beams of 78-ps (FWHM), up to 1-J pulses at 1064 nm and 10 Hz repetition rate. Pulses at 532 nm are generated via type-II second-harmonic generation (SHG) of two fundamental 1064 nm beams in a 10 mm long DKDP crystal. The remaining fundamental and a part of the SH are relay-imaged with vacuum telescopes onto a 10 mm long DKDP crystal for type-II sum-frequency generation (SFG). Usually, 6 mJ at 532 nm and 14 mJ at 1064 nm are used to generate 8 mJ pulses of the third-harmonic (TH) at 355 nm. The beam diameters are 5 mm each. A high energy conversion efficiency of 40% and a quantum efficiency of 90% with respect to the SH is observed. The SH and TH pump pulse durations are also approximately 78 ps due to the strong saturation in the conversion.

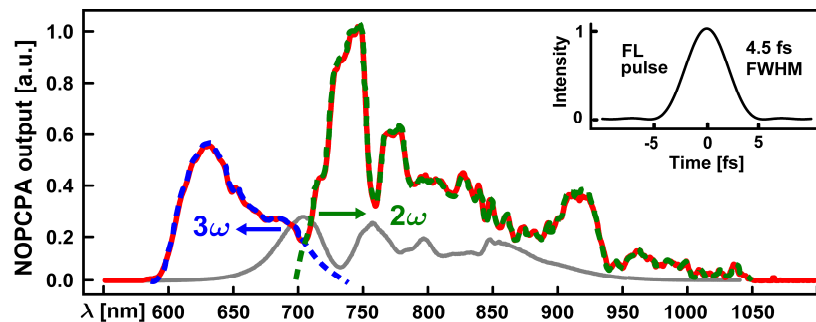


Fig. 2. The spectral energy density of the signal pulse amplified by the second-harmonic and the third-harmonic of the Nd:YAG pump laser (575-1050 nm, red solid curve) allows for a Fourier-limit of 4.5 fs (inset). This spectrum is composed of the spectral region amplified only by the second-harmonic (700-1050 nm, green dotted curve shown as guide to the eye) and the third-harmonic alone (575-740 nm, blue dotted curve). A typical output spectrum of the T-HCF (unamplified seed, not to scale) is shown as gray solid curve.

The first NOPCPA stage (calculated phase-matching angle $\theta = 23.62^\circ$, internal noncollinear angle $\alpha = 2.23^\circ$) consists of a 5 mm long type-I BBO crystal with a slight wedge to avoid adverse effects of internal reflections [9]. It is pumped by 14 mJ of the SH with a 2 mm diameter of the sixth-order super-Gaussian beam and a peak intensity of about $10 \text{ GW}/\text{cm}^2$. The second NOPCPA stage ($\theta = 34.58^\circ$, $\alpha = 3.40^\circ$) consists of a 3 mm long type-I BBO crystal and is pumped by 7 mJ of the TH with 1.5 mm diameter and a peak intensity of close to $10 \text{ GW}/\text{cm}^2$. Both stages are operated in tangential phase-matching geometry, both pump beams being relay-imaged onto the crystals and being slightly smaller than the seed beam so as to achieve a good spatial signal beam profile. With a group delay of 37 ps for the full seed bandwidth, the seed is amplified from 700 to 1050 nm to an energy of 1.4 mJ in the first stage and further amplified from 575 to 740 nm in the second stage. The particular seed delay was chosen to ensure that the full spectral range of the seed lies within the pump pulse duration. The very high small signal gain of OPCA allows utilization of the exponentially decreasing seed light at the spectral edges. Overall, an output energy of 1.9 mJ and a spectrum spanning from 575 to 1050 nm is achieved. This nearly octave-wide spectrum supports a Fourier limited pulse of 4.5 fs (see inset in Fig. 2). The results from the seed GD variation are discussed in section 4.1. The positively chirped pulses do not allow the use of the available pulse compressor and hence restrict us to a spectral characterization of the pulses.

3. Proof-of-principle compressibility with high-repetition rate NOPA on the μJ -level

Figure 3 shows the layout for the μJ -level, high-repetition rate NOPA setup. As primary pump laser we use a commercial diode-pumped Yb:KYW disc laser system (JenLas® D2.fs,

Jenoptik AG), delivering 300-fs, 40- μ J pulses at a center wavelength of 1025 nm and a repetition rate of 100 kHz. For generating the seed we split off approximately 1.5 μ J of energy and focus it (all focal lengths are given in Fig. 3) onto a 2 mm thick YAG plate, where a supercontinuum ranging from 470 nm to above 1 μ m results [19]. The main part of the pump pulses is focused towards two BBO crystals, where type-I SHG and subsequent type-II SFG are performed in a simple collinear arrangement [18]. In this way we obtain pulses with an energy of 13.5 μ J at the SH and 7.5 μ J at the TH, which are separated by dichroic mirrors and independently collimated with fused silica lenses. The supercontinuum is collimated with a thin fused silica lens and fed into the first NOPA stage ($\theta = 24.0^\circ$, $\alpha = 2.3^\circ$), which consists of a 3 mm long type-I BBO crystal. The first NOPA stage is pumped by the SH, whose energy can be adjusted by a combination of half-wave-plate and polarizer.

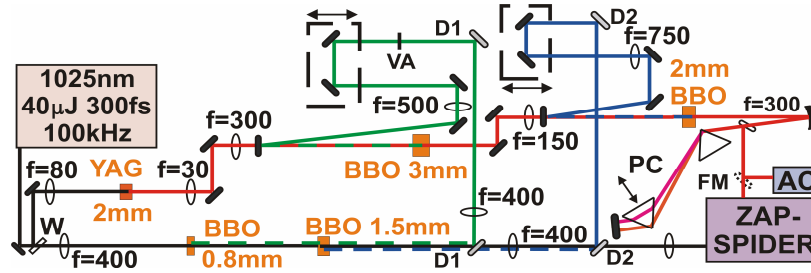


Fig. 3. Layout of the two-color-pumped NOPA setup, which consists of two cascaded stages employing type-I phase-matching in BBO (W - fused silica window, D - dichroic mirror, VA - variable attenuator, PC - prism compressor, FM - flipper mirror, AC - 2nd-order intensity autocorrelator). All focal lengths f are given in mm.

To achieve the necessary pump intensities for a high gain in the NOPA process, focusing of the pump beams and consequently focusing of the seed beams towards the nonlinear crystals is inevitable with this low-energy system, in contrast to the system described above. To achieve a good beam profile with a homogenous spectral distribution after both amplification stages, we find that proper matching of the divergence of pump and seed in both stages is crucial. For this reason we measured the divergence of all relevant beams around the position of the nonlinear crystals with a CCD camera and carefully selected and determined the focal lengths and positions of the respective focusing lenses. The amplified signal of the first stage was then 1:1 relay-imaged onto the BBO crystal (2 mm, type-I) of the second NOPA stage ($\theta = 35.5^\circ$, $\alpha = 2.7^\circ$), which is pumped by the TH.

In each stage special care has to be taken to spatially overlap the amplified signal beam with the respective seed beam, which is not ensured automatically. We have observed, that only in case of the geometry with the pump polarization oriented in the plane defined by seed and pump, spatial overlap of amplified signal and seed can be achieved. Additionally, the BBO crystal had to be set up to Poynting-vector walk-off configuration. We conclude, that the birefringent nature of the BBO crystal and the corresponding pump walk-off can compensate the shift of the amplified signal with respect to the seed direction. In the original design of the NOPA the noncollinear seed pump interaction is arranged in a vertical plane, the polarization of the seed is horizontal and that of the pump vertical [6,7]. Many setups use a horizontal geometry for practical reasons. If the seed is polarized vertical and the pump horizontal in this arrangement, no physical difference originates [8,12,20]. For the horizontal seed polarization and the vertical pump polarization used by us, we explicitly compared the vertical and horizontal pump seed interaction geometry. We found that only for the vertical beam geometry, a proper overlap of seed and signal could be achieved. Slight deviations from the optimum noncollinear and/or phase-matching angle had to be accepted.

We amplify spectral regions from 690 to 830 nm with the second harmonic and from 630 to 715 nm with the third harmonic (Fig. 4(a)). Due to the relatively short pump pulses (estimated to be 220 fs for the SH and 180 fs for the TH) in comparison to the chirped

supercontinuum seed (close to 1 ps), the amplified bandwidth is determined by the temporal overlap of pump and seed, and not the phase-matching bandwidth of the crystals. Variation of only the seed pump delay results in a shift of the spectrum. With a seed energy of 2 nJ, typical output energies are 1 μ J for the first stage when pumped with 9.3 μ J (200 μ m diameter, peak intensity of 250 GW/cm²) and 350 nJ for the second stage when pumped with 6.0 μ J (205 μ m diameter, peak intensity of 190 GW/cm²). The lower efficiency of the second stage is believed to be due to the group velocity mismatch between the UV pump and the visible seed. Both stages operating together typically yield a higher output energy (1.8 μ J) than the sum of the single stages. This is due to the fact that part of the amplified spectrum in the first stage overlaps with the amplification bandwidth of the second stage and therefore acts as a stronger seed than the supercontinuum alone, eventually leading to saturation in the second stage, as is also visible in the signal spectra shown in Fig. 4(a).

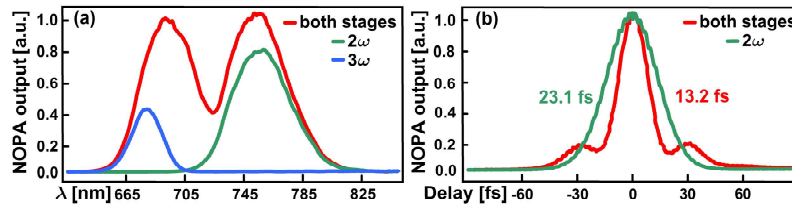


Fig. 4. (a) The spectral energy density of the signal pulse amplified by the SH and the TH of the pump laser (630 – 830 nm, red curve) is composed of the spectral region amplified only by the SH (690 – 830 nm, green curve) and the TH alone (630 – 715 nm, blue curve). These spectra allow for Fourier-limits of 11 fs, 19.7 fs and 28 fs, respectively. The measured spectral energy densities are normalized to the peak of the red curve. The corresponding measured autocorrelation traces with deconvoluted FWHM pulse durations are shown in (b).

After the two amplification stages the output signal is collimated with a spherical mirror and compressed using a sequence of fused silica prisms with an apex angle of 68.7°. Characterization of the pulses is performed online with a dispersion-free autocorrelator that provides direct information in the time domain [21] and alternatively with a ZAP-SPIDER setup that characterizes the pulses in the spectral domain [22]. We use a 30 μ m thin BBO crystal for both devices. As auxiliary pulse for the ZAP-SPIDER we use the residual fundamental at 1025 nm after SHG and SFG, which is stretched by transmission through 1270 mm SF57 glass to a FWHM duration of 1.4 ps.

4. Results and discussion

4.1 NOPCPA on the mJ-level approaching the octave

The amplified signal spectrum in case of the mJ-level, cascaded two-color-pumped NOPCPA, which is outlined in section 2, ranges from 575 to 1050 nm with a total confined energy of 1.9 mJ. The pulse has a Fourier-limit of 4.5 fs (FWHM duration, see Fig. 2 inset) and a central wavelength of 782 nm. The spectral boundaries are determined by the effective phase-matching bandwidth shown in Fig. 5(a). The effective phase-mismatch in a BBO crystal of length L is calculated according to Ref. [15] as the sum of crystal-dependent wavevector-mismatch ΔkL and amplification-dependent OPA-phase (Eq. (8) in Ref. [15]). ΔkL leads to a phase-slippage between the pump wave, the seed wave and the idler wave generated in the BBO. The OPA-phase is a phase imprinted on the signal during amplification so as to compensate for the phase-slippage and therefore maintain high gain even in areas of significant ΔkL [15]. A maximum effective phase-mismatch of $\pm\pi$ is acceptable for coherent build-up of the amplified signal in the small-signal gain regime. The compensating effect of the OPA-phase broadens the acceptance bandwidth. In our experiment, the amplified bandwidth in the NOPCPA stage pumped by the SH matches exactly the calculated one shown in Fig. 5(a). In case of the TH-pumped stage, the measured amplified bandwidth is

even slightly broader. This may be because Eq. (8) in Ref. [15] is only valid for low pump depletion.

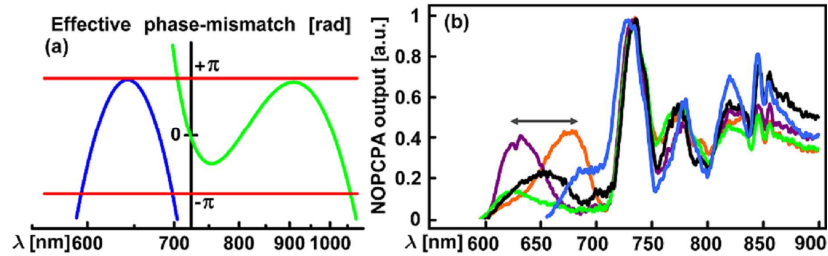


Fig. 5. (a) Effective phase-mismatch as function of seed wavelength including wave-vector-mismatch ΔkL and OPA-phase for the individual NOPCPA stages: $\lambda_p = 532$ nm, $\theta = 23.62^\circ$, $\alpha = 2.23^\circ$ (green) and $\lambda_p = 354.7$ nm, $\theta = 34.58^\circ$, $\alpha = 3.40^\circ$ (blue). The red horizontal lines label $\pm\pi$. (b) The spectral region below 700 nm is shapeable via adjusting the pump delay and the phase-matching angle (varied colors) in the NOPCPA stage pumped by 3ω .

Figure 5(b) shows a cut-out of signal spectra obtained through amplification by the SH and the TH. A steep spectral edge at around 700 nm leads to satellite pulses in the time domain after almost Fourier-limited compression [12], potentially degrading the temporal pulse contrast on the femtosecond timescale. This can be avoided by spectral shaping of the region below 700 nm via adjusting the pump delay and phase-matching angle in the NOPCPA stage pumped by the TH. Consequently, if one achieves adaptive compression of this octave-spanning pulse close to the Fourier-limit, optimization of the temporal structure of the compressed pulse seems to be possible via spectral shaping in the NOPCPA stages. The spectral structure above 700 nm in the signal spectrum in Fig. 2 is mainly dominated by modulation of the unamplified seed, which is spectrally broadened via self-phase modulation in the tapered hollow-core capillary fiber filled with neon gas.

It has been predicted that the overall pump-to-signal conversion efficiency and the full signal bandwidth of a NOPCPA are functions of group delay of the seed spectral boundaries [23]. Measured results for our cascaded two-color-pumped NOPCPA are summarized in Fig. 6 and represent to our knowledge the first reported measurement. Figure 6 shows that a variation from the seed GD of 37 ps, which is chosen for most of the measurements, can improve the conversion efficiency even further. A GD of (69 ± 2) ps for 575 to 1020 nm leads to the highest overall conversion efficiency of $(12.5 \pm 1.3)\%$, while still maintaining the signal bandwidth. The GD for 700 to 1020 nm and for 575 to 740 nm is roughly 33 ps and 43 ps, respectively. In this case, the conversion efficiency is 14.4% and 8.8% in the NOPCPA stages pumped selectively by the SH and the TH, which is the highest conversion efficiency obtained for the SH-pumped stage. In the SH-pumped stage, the pump energy is 16 mJ and the signal energy is 2.3 mJ. For the TH-pumped stage, the corresponding energies are 8 mJ and 0.7 mJ, yielding a total output energy of 3 mJ. Hence, both stages are operated near saturation. At the experimentally verified optimum seed GD, the results show a signal spectrum in the SH-pumped stage similar to that in Ref. [12] but with higher conversion efficiency, although the seed GD for 700 to 1020 nm is similar in both cases. We suspect that this is because we do not use an acousto-optic modulator (Dazzler) in the unamplified seed beam and for this reason observe a spatially and spectrally more homogeneous unamplified seed beam profile in the present experiment.

In general, the temporal overlap between the seed pulse and the 78 ps (FWHM) pump pulse increases with increasing seed GD until the optimum GD is reached. In this range, the conversion efficiency grows and the signal bandwidth stays constant as long as the NOPCPA stage is operated near saturation for most of the seed wavelengths. Otherwise, a decrease in seed intensity because of an enhanced stretching ratio can lead to lower signal bandwidth due to a lack of saturation [23]. Beyond the optimum GD, the seed pulse increasingly experiences the Gaussian temporal shape of the pump pulse, leading to a decrease in signal bandwidth and conversion efficiency.

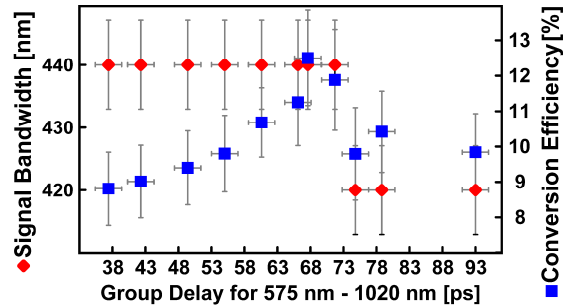


Fig. 6. Measured full signal bandwidth (red diamonds) and the overall pump-to-signal conversion efficiency (blue squares) as function of group delay between the seed spectral boundaries. The optimum group delay is found to be (69 ± 2) ps.

In conclusion, with a proper and precise dispersion management, two-color-pumped NOPCPA with type-I phase-matching in BBO is a promising approach for the generation of sub-two-cycle light pulses on the mJ-level. In this case, the present technique would close the gap between chirped-pulse amplifiers with HCFs (~ 4 fs, ~ 1 kHz, ~ 1 mJ [24,25]) and few-cycle one-color-pumped NOPCPA systems (~ 8 fs, ~ 10 Hz, 15-130 mJ [11,12]).

4.2 Proof-of-principle compressibility with high-repetition rate NOPA on the μJ -level

The amplified signal spectrum in case of the μJ -level cascaded two-color-pumped NOPA described in section 3 ranges from 630 to 830 nm with a total confined energy of 1.8 μJ . The spectral overlap is chosen to be similar to that in the mJ-level NOPCPA setup in section 2, with a central wavelength of 740 nm. Figure 4 shows the amplified spectrum and the corresponding measured autocorrelation trace (both in red). With identical prism compressor settings, we measure a FWHM pulse duration of 23.1 fs (Fourier-limit: 19.7 fs) and 95.0 fs (Fourier-limit: 28.0 fs) for the signal pulse amplified only by the SH and only by the TH. The signal pulse amplified in both stages is compressed to 13.2 fs, compared to its Fourier-limit of 11.0 fs. The measurement matches the simulation of our prism compressor and the compressibility is comparable to other experiments employing related prism compressors [20,26].

The prism compressor setting for optimum compression of the signal pulse resulting from amplification in both NOPA stages is also the optimum setting for the signal pulse amplified by the SH alone, in contrast to the signal amplified by the TH alone. To compress the signal amplified in the TH-pumped stage, the second prism of the compressor is further inserted. Consequently, less negative GDD is required if the signal amplified in the TH-pumped stage is to be compressed. During the course of the experiments, a deformable mirror as prism compressor end-mirror was sometimes found to reduce the outer wings of the compressed pulse.

A more detailed understanding can be gained from the determination of the spectral phase of the amplified pulse. Figure 7(a) shows the result of a ZAP-SPIDER [22] measurement for a particular pulse with a total amplified range of 615 to 780 nm. Figure 7(b) shows the amplified and compressed pulses calculated from the measured spectral intensity and phase given in Fig. 7(a). The FWHM pulse durations determined in this way are close to the results obtained with autocorrelation measurements of the same pulses.

The compressibility is determined by three factors. First, the bandwidth, whose phase can be managed throughout the present dispersive bulk materials (YAG and BBO crystals, fused silica lenses) and the fused silica prism-compressor, is limited. In case of the optimum compressor setting for the investigated spectral region a nearly vanishing spectral phase over a wide range results. The GD as a function of the signal wavelength shows a maximum around 710 nm, which limits the bandwidth of the compressed pulse. Furthermore, the third-order dispersion (TOD) due to the dispersive components leads to satellite pulses after compression.

These limitations mean that the spectral components below 660 nm and above 800 nm occur in the wings of the compressed pulse for the case of Fig. 4. This is responsible for the observation of the long pulse durations seen when the signal is amplified only by the TH. Nevertheless, the TH-pumped stage amplifies spectral components not amplified in the SH-pumped stage and whose phase can still be managed in our case using the prism compressor. For this reason, a shorter pulse duration is achieved in case of amplification in both NOPA stages compared to using only the SH-pumped stage, for the same prism compressor settings.

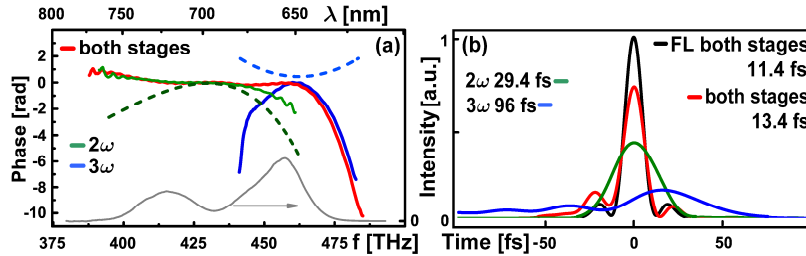


Fig. 7. (a) Spectral phase of the compressed signal pulses retrieved by the ZAP-SPIDER measurement. Solid red curve: amplification by the SH and TH of the pump laser, solid green: amplification only by the SH, solid blue: amplification only by the TH; all for identical settings of the compressor. For comparison the calculated OPA-phase for the two stages is shown with dashed lines. The solid grey curve shows the spectral energy density of the signal. Taking the measured spectral phase, spectral intensity and pulse energy leads to the retrieved pulses shown in (b) with their FWHM pulse duration.

Second, the phase imprinted on the signal to compensate for phase-mismatch and to maintain high gain (OPA-phase) comes into play [27]. As mentioned in subsection 4.1 and outlined in Ref. [15] and Ref. [28], this phase contribution affects ultra-broadband optical parametric amplification. Employing Eq. (8) of Ref. [15] for the case of small depletion, these phase contributions due to amplification in the TH-pumped and the SH-pumped NOPA stages are shown as dashed lines in Fig. 7(a) for the experimentally determined parameters like crystal angles and the pump intensities. One can see that the phase contributions have opposite signs. A positive linear chirp defined in the time domain leads to a parabola with a negative second derivative in the frequency domain via Fourier-transformation. In contrast to the SH-pumped NOPA stage, the phase imprinted on the signal during parametric amplification by the TH shows negative group delay dispersion (GDD). This matches our observation that less negative GDD was required with the prism compressor when the signal pulse was amplified by the TH alone. Moreover, these two phase contributions partially compensate each other and therefore lead to an extended region of reduced residual phase around the spectral overlap.

To experimentally verify this phase effect, we adjusted both NOPA stages to similar amplified spectra centered at 670 nm (different from the pulses previously described) and subsequently compressed the signal pulse amplified by each stage separately with the same prism compressor spacing. These compressed pulses were characterized with the autocorrelator. It was found that for optimum compression of the signal pulse amplified in the TH-pumped NOPA stage, the second prism in the compressor was inserted by about 2 mm more compared to the signal amplified in the SH-pumped stage. This implies that the prism compressor applies less negative GDD to the signal pulse, which matches the signs of the OPA-phase contributions due to parametric amplification shown in Fig. 7(a).

Note that the residual phase of the compressed signal pulse amplified by the SH or the TH alone is different from the residual phases of the corresponding spectral regions in case of amplification in both NOPA stages. Apart from the compensating effect of the phase-contribution due to parametric amplification in the region of spectral overlap, this occurs because Eq. (8) in Ref. [15] is strictly speaking only valid for the case of low pump depletion (i.e. negligible saturation). This observation has the consequence that the two amplification stages and the pulse compression can only be optimized simultaneously.

Third, cross-phase modulation (XPM), which is possible in optical parametric amplification as a result of the high pump intensities, would lead to positive GDD [29]. According to Ref. [29], we calculate the B-integral due to XPM in our NOPA stages to be 1.4 rad in the SH-pumped and 0.8 rad in the TH-pumped stages. This is comparable to the value found in the investigation of XPM [29]. Since the B-integral of the SH-pumped stage is approximately twice as high as that of the TH-pumped stage, a higher additional positive GDD can be present in the SH-pumped stage. This is consistent with our observations.

In conclusion, cascaded two-color-pumped NOPA with type-I phase-matching in BBO is also a promising approach for the generation of sub-two-cycle light pulses on the μJ -level in high-repetition rate NOPA systems.

5. Conclusion and perspectives

In this work results from two novel experimental setups were analyzed to investigate the feasibility of two-color pumping of a NOPCPA for the generation of high energy pulses approaching the single cycle regime. At low repetition rates, 3 mJ pulses with a nearly octave wide spectrum were demonstrated in a first double-stage arrangement. At 100 kHz repetition rate and μJ output energies the spectral phase and compressibility was studied. The two-color scheme exhibits a slowly and continuously varying spectral phase that should be well compensatable with existing compression schemes. The addition of the visible part of the pulse spectrum by the 3ω -pumping indeed shortens the pulse by nearly a factor of two without any change to the prism compressor. We conclude from the combination of results that the concept of two-color pumping can be expanded to multiple stages. Proper care has to be taken in the design and alignment to utilize the full available pump energy. Pulses approaching a J energy and a duration around 5 fs seem on the horizon. While sub-5s pulses were previously reported with 400 nm Ti:sapphire based pumping, this range is now reachable with the 1050 nm pump lasers of much higher energy.

Various challenges have to be resolved to achieve these ambitious goals. Already in the present experiments matching of the wavefront and beam pointing of the two contributions to the composite pulses needed high attention. We suspect that the birefringent nature of the amplifier crystals, possible inhomogeneities in the material, partial depletion of the pump and associated spatially-dependent OPA phase and classically neglected higher-order nonlinear interactions are the main causes of this situation. The OPA phase will depend selectively on the pump color, the degree of saturation and therefore on the OPA's location within an extended amplifier chain, and on the particular phase-matching adjustment of a selected crystal. Therefore an adaptive phase-correction will most likely be desirable for routine operation. An acousto-optic programmable dispersive filter with sufficient bandwidth is already available. Last but not least, the correct stretching ratio of seed and pump for the optimum balance of bandwidth, compressibility and overall efficiency is of high importance. For all these issues the present report provides a first basis.

Two-color pumping potentially allows more efficient usage of the available pump energy. Only for the short wavelength part of the output spectrum are the "expensive" short wavelength pump photons used, while the red part of the spectrum is amplified with the help of the remaining green pump light. Already now the generation of the UV pump utilizes the fundamental pump pulses twice. In future extensions of the concept one could even think of adding another amplifier stage pumped by the residual pump fundamental to widen the spectrum in the near infrared and to add even more energy.

It is interesting to compare the optical principles underlying the present approach for the generation of extremely broadband pulses with other methods of light wave synthesis. Recently it was demonstrated that interferometric spatial addition of phase-locked pulses generated at neighboring wavelength ranges in a fiber-based MHz system leads to single cycle near-infrared pulses [30]. This approach of individual amplification and dedicated compression of the spectral parts allows for more flexibility. On the other hand, the spatially and temporally stable overlap of the contributions, without adverse effects from inhomogeneities in scaling to high pulse energies and consequently large beam sizes, might be

critical. In our approach a common seed and beam path is used and could eventually be more practical.

The motivation for our work was the high energy, low repetition rate regime. In the course of the work we realized that two- or even multiple color pumping for the extension of the output spectrum is also feasible at 100 kHz repetition rates. This might provide interesting sources for spectroscopic investigations of samples in the condensed phase that require only low pulse energies. It is certain that the concept can close existing gaps between Ti:sapphire based systems with hollow-core capillary-fiber compression (~ 4 fs, ~ 750 nm, ~ 1 mJ, ~ 1 kHz [24,25]) and 8 fs, 800 nm, 10 Hz, 15-130 mJ NOPCPA systems [11,12].

Acknowledgements

This work was supported by Deutsche Forschungsgemeinschaft (contract TR18), the association EURATOM-Max-Planck-Institut für Plasmaphysik, the Cluster of Excellence Munich-Centre for Advanced Photonics (MAP) and by the Austrian Science Fund within the Special Research Program F16 (Advanced Light Sources). We acknowledge support by the cooperation with the King-Saud-University. D. H. is grateful to the Studienstiftung des deutschen Volkes. The International Max Planck Research School on Advanced Photon Science (C. H.) is gratefully acknowledged. The authors thank N. Krebs for valuable support during the SPIDER measurements.